

Supplementary Information: Iron oxide  
xerogels for improved water quality  
monitoring of arsenic(III) in resource-limited  
environments via solid-phase extraction,  
preservation, storage, transportation, and  
analysis of trace contaminants (SEPSTAT)

Michael S. Bono Jr., Emily B. Hanhauser, Chintan Vaishnav,  
A. John Hart, and Rohit Karnik

## Contents

<b>S1 Reagents and materials</b>	<b>S-2</b>
<b>S2 Xerogel fabrication process</b>	<b>S-3</b>
<b>S3 Isotherm and adsorption capacity calculation methodology</b>	<b>S-4</b>
<b>S4 Methods and results for preliminary experiments</b>	<b>S-5</b>
S4.1 Representative arsenic(III) adsorption isotherms at neutral and high pH values . . . . .	S-5
S4.2 Recovered arsenic concentration after extraction in 100 mM sodium hydroxide . . . . .	S-9
S4.3 Arsenic adsorption and recovery efficiencies as a function of xerogel loading in different adsorption test solutions . . . . .	S-9
<b>S5 Particle size analysis for pulverized xerogels</b>	<b>S-11</b>
<b>S6 Detection limit calculation methodology</b>	<b>S-14</b>
<b>S7 Tabulated method performance evaluation measurements</b>	<b>S-15</b>
<b>S8 Xerogel bill of materials and cost calculation</b>	<b>S-16</b>

## List of Tables

S-1	Fitted isotherm model parameters for representative arsenic(III) adsorption isotherms . . . . .	S-8
S-2	Test solutions used for investigation of the effects of xerogel loading . . . . .	S-10
S-3	Initial and recovered arsenic concentrations for arsenic adsorbed from Low Mix test solutions . . . . .	S-15
S-4	Initial and recovered arsenic concentrations for arsenic adsorbed from High Mix test solutions . . . . .	S-15
S-5	Xerogel bill of materials and cost calculation . . . . .	S-16

## List of Figures

S-1	Representative arsenic(III) adsorption isotherms at neutral and high pH values . . . . .	S-7
S-2	Recovered arsenic concentration as a function of initial arsenic concentration for extraction with 100 mM sodium hydroxide .	S-9
S-3	Arsenic adsorption and recovery efficiencies as a function of xerogel loading . . . . .	S-11
S-4	Microscope images of pulverized xerogels used for particle size analysis . . . . .	S-12
S-5	Particle size distribution of pulverized xerogels . . . . .	S-13

## S1 Reagents and materials

We synthesized iron oxide xerogels from iron chloride hexahydrate,  $\text{FeCl}_3 \cdot 6 \text{H}_2\text{O}$  (puriss. p.a., Reag. Ph. Eur.,  $\geq 99\%$ ,  $\leq 5 \text{ mg/kg As}$ , Sigma-Aldrich); propylene oxide (puriss. p.a.,  $\geq 99.5\%$ , Sigma-Aldrich); and absolute ethanol (200 proof, Molecular Biology Grade, Fisher Scientific). Sodium arsenite solution,  $\text{NaAsO}_2$  (0.1 N Standardized Solution, Alfa Aesar), was selected as an arsenic(III) source for adsorption due to its previous use in investigation of arsenic adsorption by iron oxides.<sup>1</sup> In addition, adsorption and extraction solutions were prepared from sodium chloride (BioXtra,  $\geq 99.5\%$ ,  $\leq 1 \text{ mg/kg As}$ ); sodium nitrate (BioUltra,  $\geq 99.0\%$ ,  $\leq 0.1 \text{ mg/kg As}$ ); sodium sulfate decahydrate (BioUltra,  $\geq 99.0\%$ ,  $\leq 0.1 \text{ mg/kg As}$ ); sodium phosphate monobasic dihydrate,  $\text{NaH}_2\text{PO}_4 \cdot 2 \text{H}_2\text{O}$  (BioUltra,  $\geq 99.0\%$ ,  $\leq 0.2 \text{ mg/kg As}$ ); sodium phosphate dibasic dihydrate,  $\text{Na}_2\text{HPO}_4 \cdot 2 \text{H}_2\text{O}$  (BioUltra,  $\geq 99.0\%$ ,  $\leq 0.1 \text{ mg/kg As}$ ); sodium phosphate tribasic dodecahydrate,  $\text{Na}_3\text{PO}_4 \cdot 12 \text{H}_2\text{O}$  (puriss. p.a.,  $\geq 98.0\%$ ,  $\leq 1 \text{ mg/kg As}$ ); sodium bicarbonate (BioXtra,  $\geq 99.5\%$ );

sodium metasilicate nonahydrate,  $\text{Na}_2\text{SiO}_3 \cdot 9 \text{H}_2\text{O}$  ( $\geq 98\%$ ); and sodium hydroxide (BioUltra,  $\geq 98.0\%$ ,  $\leq 0.1 \text{ mg/kg As}$ ), all purchased from Sigma-Aldrich.

Hydrochloric acid (TraceMetal Grade,  $\leq 0.5 \text{ ppb As}$ , Fisher Scientific) was used for solution pH adjustment and acid-washing. Nitric acid,  $\text{HNO}_3$  (TraceMetal Grade,  $\leq 0.5 \text{ ppb As}$ , Fisher Scientific), was used to acidify samples for ICP-MS and ICP-AES analyses, as well as for use in the ICP-AES rinse solution. Analytical standards were prepared using  $1000 \mu\text{g/mL}$  standards of arsenic (in  $2\% \text{ HNO}_3$ , for ICP/MS, Claritas PPT Grade), phosphorus (in  $\text{H}_2\text{O}$ , for ICP), and silicon (in  $\text{H}_2\text{O}$ , for ICP), all from SPEX CertiPrep, as well as  $10,000 \mu\text{g/mL}$  indium (in  $5\% \text{ HNO}_3$ ) from Inorganic Ventures. ICP-MS rinse solution was prepared from ultrapure nitric acid (max.  $20 \text{ ppt As}$ ) and hydrochloric acid (max.  $50 \text{ ppt As}$ ), both BDH Aristar Ultra (VWR International). All water used for solution preparation was purified to  $18.2 \text{ M}\Omega\text{-cm}$  resistivity using a Milli-Q purification system (Millipore).

Adsorption solutions, extraction solutions, and analytical standards were prepared in borosilicate glassware and stored in either high-density polyethylene bottles (Nalgene) or polypropylene centrifuge tubes (VWR International). Glassware and polyethylene bottles were acid-washed before each use by submerging in  $10\% \text{ HCl}$  for at least two hours. Xerogel gelation occurred in  $100 \text{ mm} \times 20 \text{ mm}$  nontreated polystyrene culture dishes (Corning).

## S2 Xerogel fabrication process

Iron oxide xerogels were fabricated using an epoxide-assisted sol-gel synthesis method adapted from Gash *et al.*<sup>2</sup> First,  $6.487 \text{ g FeCl}_3 \cdot 6 \text{H}_2\text{O}$  was dissolved in  $52.5 \text{ mL}$  ethanol while stirring in a water bath. Once the  $\text{FeCl}_3 \cdot 6 \text{H}_2\text{O}$  was fully dissolved,  $18.06 \text{ mL}$  propylene oxide was added and stirring continued for a few minutes as solution color darkened from orange to a deep red. Solution was then pipetted into culture dishes and allowed to gel over a period of 30 minutes. The culture dishes were then sealed with parafilm and the gel was allowed to age over a period of 24 hours.

At the conclusion of gel aging, five ethanol solvent exchanges were conducted in order to remove residual propylene oxide and other organic impurities present after gelation.<sup>3</sup> For each solvent exchange, absolute ethanol was pipetted onto the gel ( $10 \text{ mL}$  ethanol for gel prepared from a solution volume of  $14.4 \text{ mL}$ ), which was then sealed and allowed to sit for 24 hours before solvent was removed and replaced with fresh ethanol until the end of the final solvent exchange, at which point the culture dishes were left unsealed and the

xerogels dried at ambient conditions for at least 10 days before use. Safety note: propylene oxide is highly flammable and volatile. For safe handling, chill the propylene oxide container to 0 °C before opening, prepare the sol-gel solution in a beaker placed in a water bath, and use positive-displacement pipette tips for addition of propylene oxide and transfer of sol-gel solution to culture dishes for gelation.

### S3 Isotherm and adsorption capacity calculation methodology

The equilibrium concentration of adsorbed arsenic, denoted as  $Q_e$  (mg As/g xerogel), is measured by quantifying the aqueous arsenic concentration before and after adsorption, denoted respectively as  $C_i$  and  $C_e$  (both mg As/L solution). These measured arsenic concentrations can be combined with the xerogel mass  $m_{XG}$  (g xerogel) and solution volume  $V$  (L) to determine the concentration of adsorbed arsenic:

$$Q_e = \frac{(C_i - C_e)V}{m_{XG}} \quad (1)$$

Measurements of adsorbed arsenic concentration  $Q_e$  for a range of equilibrium aqueous arsenic concentrations  $C_e$  yield an adsorption isotherm such as those presented in Fig. S-1.

In order to measure arsenic adsorption capacity, an initial arsenic concentration of 1214 mg/L was selected based on the preliminary results discussed in Section S4.1 and adsorbed onto xerogel samples ( $N = 4$ , mean mass 23.4 mg) as described in the main article text, resulting in solutions with an average equilibrium aqueous arsenic concentration of 692 mg/L (standard deviation 23 mg/L). In order to better control for arsenic adsorption onto the sample tubes under the elevated arsenic concentrations used in the capacity measurement, the equilibrium aqueous arsenic concentration for a control sample containing no xerogel and processed through the same adsorption experiment, denoted as  $C_{e,0}$  and equal to 1207 mg/L for our measurement, was used to calculate the adsorption capacity in a modified version of the previous equation:

$$Q_e = \frac{(C_{e,0} - C_e)V}{m_{XG}} \quad (2)$$

We used eq 2 to calculate the adsorbed arsenic for each of our capacity samples, yielding an average arsenic adsorption capacity of 165 mg As/g xerogel measured at an average equilibrium aqueous concentration of 692 mg/L.

## S4 Methods and results for preliminary experiments

### S4.1 Representative arsenic(III) adsorption isotherms at neutral and high pH values

For arsenic isotherm measurements (Fig. S-1), approximately 50 mg intact xerogel flakes was weighed out in polystyrene culture dishes before the addition of 30 mL adsorption solution for a xerogel loading of 1.67 g/L. Adsorption solutions consisted of sodium arsenite diluted to 0-500 mg/L arsenic(III) in a deionized water background, with sodium hydroxide used for pH elevation. Arsenic adsorption was measured after at least 24 hours of shaking at 100 rpm on a benchtop orbital shaker. At the end of adsorption, we prepared samples for analysis by diluting them by a dilution factor of 1.5 and acidifying them with nitric acid, then quantifying arsenic via ICP-AES as described in the main article text.

Isotherms were calculated via eq 1 and fitted to the Langmuir, Freundlich, and Langmuir-Freundlich isotherm models (Fig. S-1). The Langmuir model assumes monolayer adsorption on a finite number of homogeneous adsorption sites, with adsorption capacity  $Q_{max}$  and uniform equilibrium constant  $K_L$ :<sup>4,5</sup>

$$Q_e = \frac{Q_{max}K_L C_e}{1 + K_L C_e} \quad (3)$$

The Freundlich model assumes multilayer adsorption on heterogeneous adsorption sites with a distribution of adsorption affinity constants.<sup>4</sup> While it is an empirical model, it can be shown to be equal to a sum of Langmuir isotherms with a lognormal distribution of equilibrium constants.<sup>6</sup> This distribution is modeled using a coefficient  $K_F$  and a dimensionless index  $n$  corresponding to the degree of heterogeneity in adsorption:

$$Q_e = K_F \times C_e^{1/n} \quad (4)$$

The combination of a finite adsorption capacity and a distribution of adsorption affinities can be modeled using the Langmuir-Freundlich model, also referred to as the Sips isotherm model.<sup>4,6,7</sup> This model retains the adsorption capacity  $Q_{max}$  and heterogeneity index  $n$  from the Langmuir and Freundlich models, respectively, combined with a baseline affinity constant  $K_{LF}$ :

$$Q_e = \frac{Q_{max}(K_{LF}C_e)^{1/n}}{1 + (K_{LF}C_e)^{1/n}} \quad (5)$$

When modeling adsorption onto a given material under different conditions where the adsorption capacity is expected to be constant, such as variations in pH, measurements under different conditions can be simultaneously fitted to Langmuir-Freundlich isotherms with a shared value of  $Q_{max}$  and different values of  $\{K_{LF}, n\}$  for each condition.<sup>7</sup>

As seen in Fig. S-1, the observed adsorption behavior was best described by a combined Langmuir-Freundlich model. The adsorbed arsenic at lower concentrations suggested a distribution of adsorption constants not able to be modeled by Langmuir isotherms (Fig. S-1a), whereas the adsorbed arsenic at higher concentrations exhibited a degree of saturation that could not be represented by the Freundlich isotherm model (Fig. S-1b). The combined Langmuir-Freundlich model, previously used to model arsenic adsorption onto iron oxide-based sorbents,<sup>4,7</sup> was able to represent adsorption behavior over the entire measured arsenic concentration range (Figs. S-1c and S-1d). The estimated parameters (Table S-1) show a decrease in estimated affinity constants ( $K_L$ ,  $K_F$ , and  $K_{LF}$ ) at pH = 13 for all three models considered and suggest that the xerogels' adsorption sites exhibit a distribution of adsorption affinities.

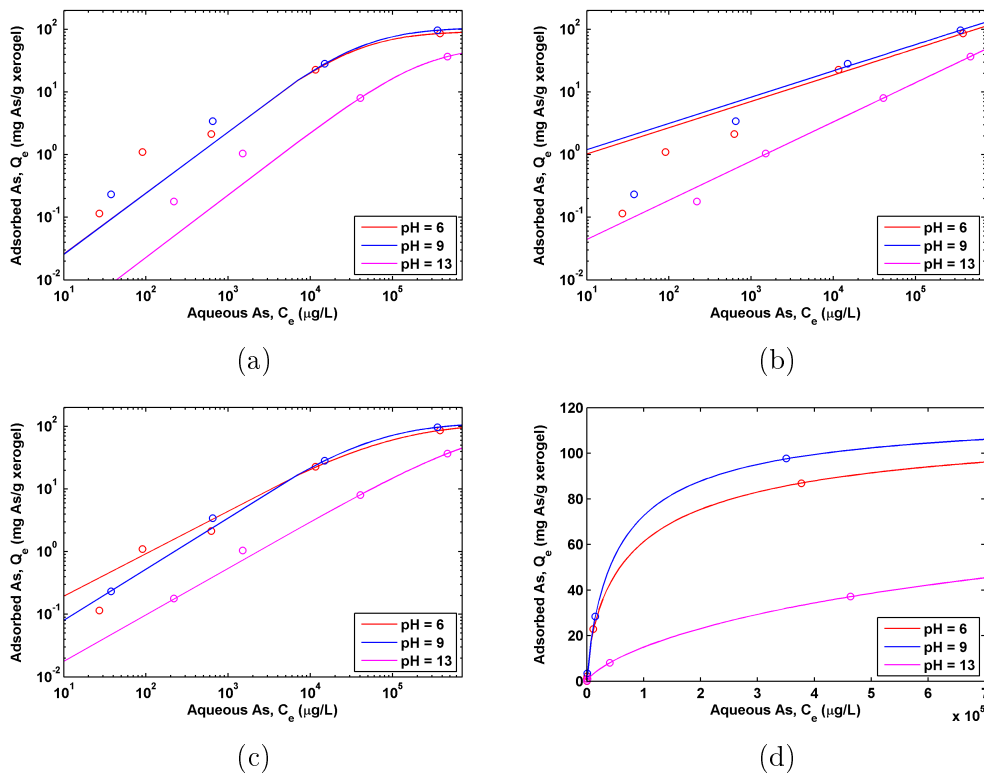


Fig. S-1: Representative arsenic(III) adsorption isotherms at neutral and high pH values, where all pH values are measured at the end of adsorption, along with fits to (a) Langmuir, (b) Freundlich, and (c,d) Langmuir-Freundlich isotherm models, with fitted parameters listed in Table S-1. Measurements at each pH are shown as points, with lines of the same color corresponding to modeled isotherms for those measurements.

Table S-1: Estimated isotherm model parameters for the representative arsenic(III) adsorption isotherms shown in Fig. S-1, along with 95% confidence intervals (95% CI) for each parameter estimate and coefficient of determination  $r^2$  for each fit. Langmuir and Freundlich parameters are for individual fits at each pH condition, whereas Langmuir-Freundlich parameters are for a simultaneous fit of all pH conditions assuming a pH-independent adsorption capacity  $Q_{max}$ . All fitting was conducted in MATLAB using the nonlinear least-squares solver `lsqcurvefit`.

Model	Parameter	pH = 6		pH = 9		pH = 13	
		Value	95% CI	Value	95% CI	Value	95% CI
Langmuir	$Q_{max}, \frac{\text{mg As}}{\text{g xerogel}}$	95	[93, 98]	109	[101, 118]	56	[45, 68]
	$K_L, \frac{\text{L}}{\mu\text{g As}}$	$2.8 \times 10^{-5}$	$[2.4, 3.1] \times 10^{-5}$	$2.4 \times 10^{-5}$	$[1.6, 3.1] \times 10^{-5}$	$4.1 \times 10^{-6}$	$[1.9, 6.4] \times 10^{-6}$
	$r^2$	0.9998		0.9995		0.9994	
Freundlich	$K_F, \frac{(\mu\text{g As})^{(1-1/n)}\text{L}^{1/n}}{\text{mg xerogel}}$	0.39	[−0.18, 0.97]	0.46	[−0.43, 1.35]	0.0105	[0.0078, 0.0131]
	$n$	2.38	[1.86, 3.28]	2.38	[1.74, 3.75]	1.60	[1.55, 1.65]
	$r^2$	0.9952		0.9965		1.0000	
Langmuir-Freundlich	$Q_{max}, \frac{\text{mg As}}{\text{g xerogel}}$	119 [105, 134]					
	$K_{LF}, \frac{\text{L}}{\mu\text{g As}}$	$1.1 \times 10^{-5}$	$[0.6, 1.6] \times 10^{-5}$	$1.7 \times 10^{-5}$	$[0.9, 2.4] \times 10^{-5}$	$7.4 \times 10^{-7}$	$[5.2, 9.6] \times 10^{-7}$
	$n$	1.42	[1.27, 1.61]	1.19	[1.01, 1.46]	1.34	[1.21, 1.50]
	$r^2$	0.9997					



## S4.2 Recovered arsenic concentration after extraction in 100 mM sodium hydroxide

Arsenic recovery via our initial extraction solution of 100 mM sodium hydroxide (Fig. S-2) was measured after adsorbing 0-5000  $\mu\text{g/L}$  arsenic(III) onto intact xerogel flakes at a xerogel loading of 1.67 g/L and an adsorption period of at least 24 hours, as described at the beginning of Section S4.1, followed by dry storage for 12 to 34 days. Arsenic was recovered over a 24 hour elution period using an extraction solution of 100 mM sodium hydroxide while shaking at 100 rpm. Recovery samples were then diluted by a dilution factor of 1.5 and acidified with nitric acid. Initial and recovered arsenic was quantified via ICP-MS as described in the main article text.

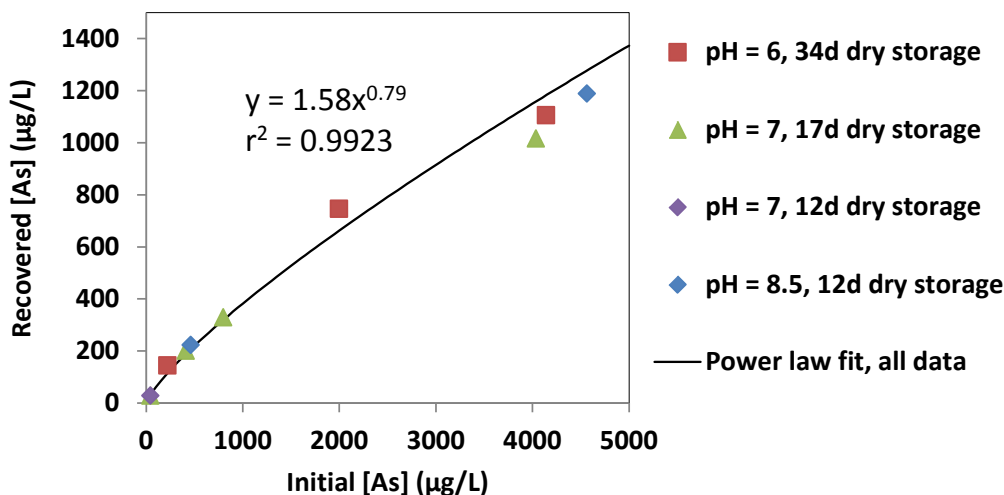


Fig. S-2: Recovered arsenic concentration as a function of initial arsenic concentration for arsenic recovered from iron oxide xerogels after adsorption from initial samples, dry storage for 12-34 days, and extraction in 100 mM sodium hydroxide, where a xerogel loading of 1.67 g/L was used for adsorption and extraction.

## S4.3 Arsenic adsorption and recovery efficiencies as a function of xerogel loading in different adsorption test solutions

Arsenic adsorption and recovery efficiencies (Fig. S-3) were measured as described in corresponding section of the main text for the adsorption test solutions listed in Table S-2, our initial extraction solution of 100 mM sodium

hydroxide, and xerogel loadings from 3.33 g/L to 13.33 g/L, where xerogel loading is defined as the mass of xerogel per volume used for adsorption and recovery. Xerogel loading was varied by weighing 25-100 mg xerogel in 15 mL polypropylene centrifuge tubes and then adding 7.5 mL of adsorption or extraction solution, and arsenic was quantified via ICP-MS as described in the main text.

Table S-2: Composition of adsorption test solutions (denoted as 2 ppm PO<sub>4</sub> Mix and 4 ppm PO<sub>4</sub> Mix) used for investigation of the effects of xerogel loading on adsorption and recovery. All concentrations are mg/L by listed species or mg/L total dissolved solids. All anions were added as sodium salts, and chloride concentrations are before addition of hydrochloric acid for adjustment to pH = 7.

Anion	2 ppm PO <sub>4</sub> Mix	4 ppm PO <sub>4</sub> Mix
Chloride (as Cl)	250	1000
Nitrate (as NO <sub>3</sub> )	45	100
Sulfate (as SO <sub>4</sub> )	200	1200
Bicarbonate (as HCO)	500	800
Silicate (as SiO <sub>2</sub> )	50	65
Phosphate (as PO <sub>4</sub> )	2.1	4.2
Total dissolved solids (TDS)	1562	4799

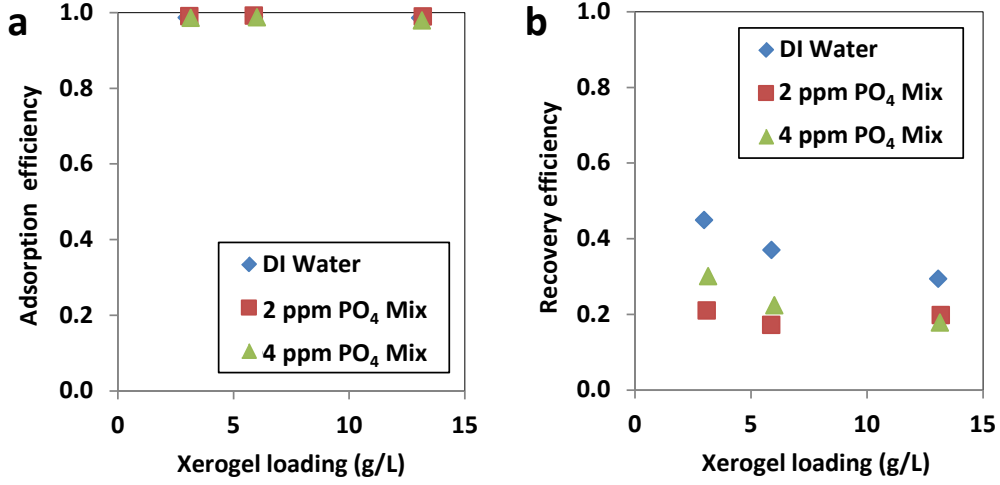


Fig. S-3: Arsenic adsorption (a) and recovery (b) efficiencies as a function of xerogel loading for adsorption from deionized water (DI Water), 2 ppm PO<sub>4</sub> Mix, and 4 ppm PO<sub>4</sub> Mix, where 2 ppm PO<sub>4</sub> Mix and 4 ppm PO<sub>4</sub> Mix are as defined in Table S-2, followed by extraction in 100 mM sodium hydroxide.

## S5 Particle size analysis for pulverized xerogels

The pulverized xerogels' particle size distribution was characterized using optical microscope images (Fig. S-4) taken with a Nikon Eclipse TE2000-U inverted microscope using a 10x objective. The diameter of representative particles ( $N = 130$ ) was measured using ImageJ software, with images of a transparent ruler used for length calibration. The measured particle diameters exhibited an average of  $109 \mu\text{m}$ , standard deviation of  $93 \mu\text{m}$ , median of  $87 \mu\text{m}$ , minimum of  $16 \mu\text{m}$ , and maximum of  $739 \mu\text{m}$ . As seen in the histograms of the measured particle diameters using linear (Fig. S-5a) and exponential (Fig. S-5b) binning, the particles exhibited a lognormal size distribution, with fitted parameters  $\theta = 4.46 \ln(\mu\text{m})$  and  $\omega = 0.66 \ln(\mu\text{m})$  for the lognormal probability density function:<sup>8</sup>

$$f(x) = \frac{1}{x\omega\sqrt{2\pi}} \exp\left[-\frac{(\ln x - \theta)^2}{2\omega^2}\right], \quad 0 < x < \infty \quad (6)$$

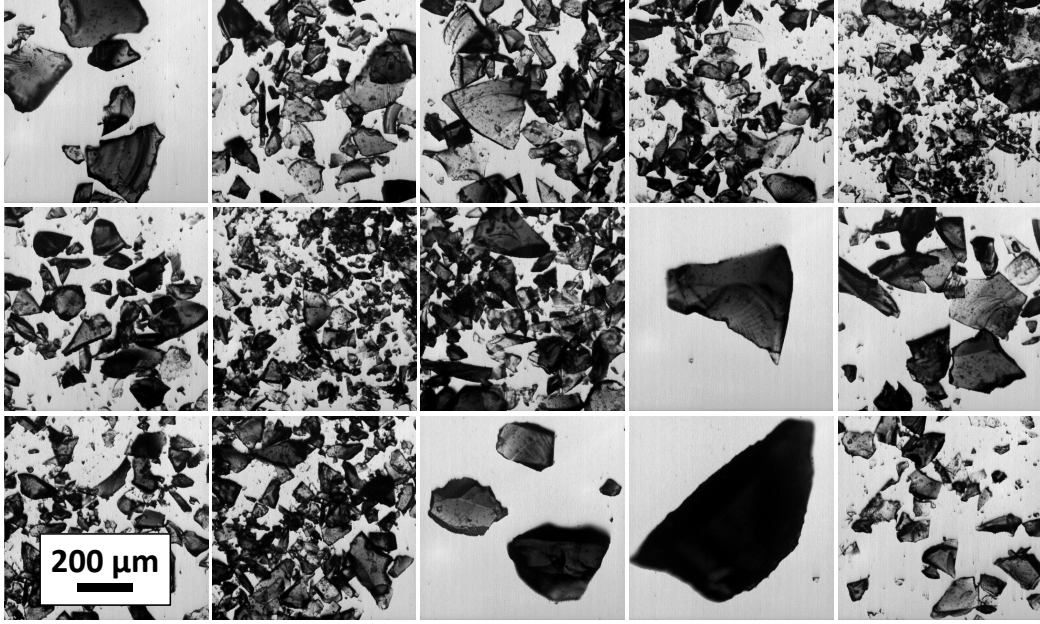
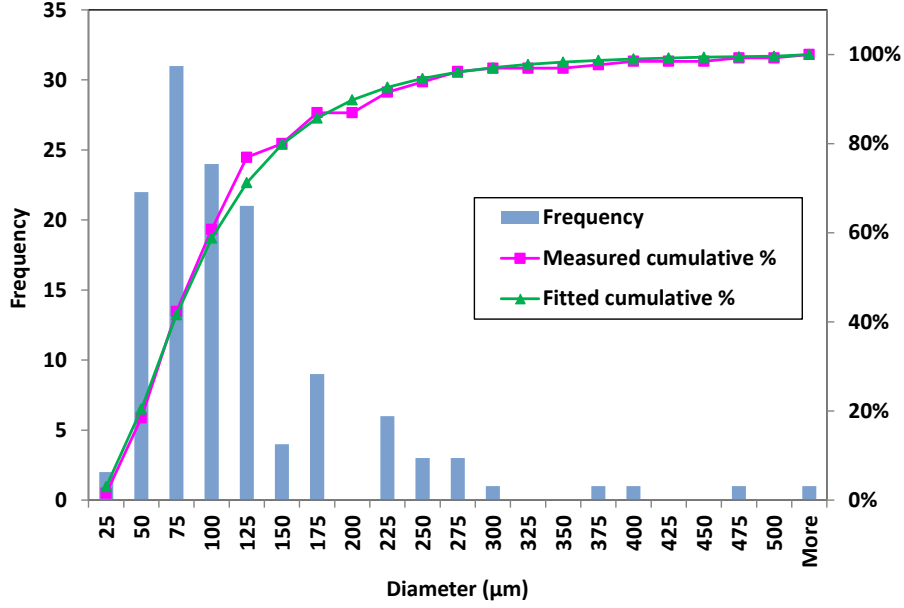
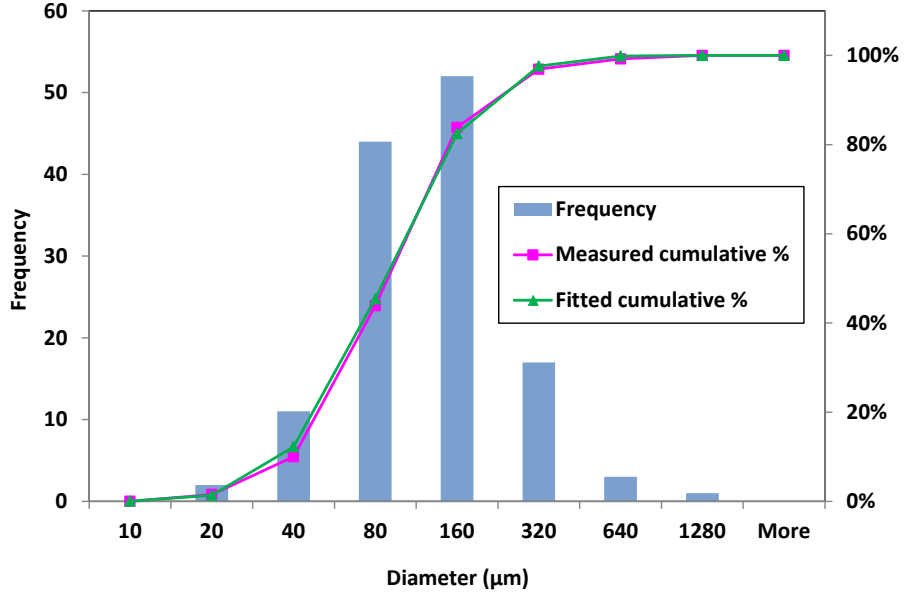


Fig. S-4: Microscope images of pulverized xerogels used for particle size analysis.

The measured lognormal particle size distribution is consistent with Kolmogorov's theory of particle breakup,<sup>9,10</sup> stating that particles during breakup will approach a lognormal size distribution if the distribution of relative particle sizes formed during breakup of a parent particle is independent of the parent particle size. That is, for parent particles of diameter  $r$ , the mean number of child particles  $Q(\alpha)$  formed with diameter  $\rho \leq \alpha r$  is a function solely of  $\alpha$  and is independent of the parent particle diameter  $r$ .



(a)



(b)

Fig. S-5: Histograms of measured particle diameters ( $N = 130$ ) for pulverized xerogel fragments with linear (a) and exponential (b) binning, along with measured and fitted cumulative percentage, where the fitted cumulative percentage corresponds to a lognormal distribution (eq 6) with fitted parameters  $\theta = 4.46 \ln(\mu\text{m})$  and  $\omega = 0.66 \ln(\mu\text{m})$ .

## S6 Detection limit calculation methodology

The detection limit (DL) for a given sample matrix was calculated as a modified version of the method detection limit (MDL).<sup>11</sup> The MDL is defined as the minimum analyte concentration which can be detected with 99% confidence that the concentration is greater than zero. Determination of the MDL requires measurement of the variation in measured concentration for a series of samples with a concentration two to three times the expected detection limit after processing through the entire analytical workflow.

For our determination of the modified MDL, we measured the variation in recovered arsenic concentration for 10  $\mu\text{g/L}$  As adsorption samples ( $N = 4$  for each sample matrix, exact measured initial arsenic concentrations in Tables S-3 and S-4) after processing through the SEPSTAT protocol with a storage period of 124-125 days. In this analytical workflow, arsenic was adsorbed onto iron oxide xerogels before dry storage at ambient conditions, followed by elution using the optimized extraction solution of 100 mM NaOH + 1 mM  $\text{Na}_3\text{PO}_4$  as described in the main article text.

The standard deviation  $\sigma_{\text{rec}}$  of the measured recovered arsenic concentrations was then multiplied by the student's t-value for a 99% confidence level (i.e. one-tailed  $\alpha = 0.01$ ) at  $n-1$  degrees of freedom (e.g.,  $t_{0.01,n-1} = t_{0.01,3} = 4.54$  for four replicates) and divided by the mean recovery efficiency  $\eta_{\text{rec}}$  for these samples in order to calculate the initial arsenic concentration which could be expected to be detected with 99% confidence:

$$\text{DL} = \frac{t_{0.01,n-1} \times \sigma_{\text{rec}}}{\eta_{\text{rec}}} \quad (7)$$

## S7 Tabulated method performance evaluation measurements

Table S-3: Initial and recovered arsenic concentrations for arsenic adsorbed from Low Mix test solutions, as defined in the main article text, recovered from iron oxide xerogels after dry storage for 125 days and extraction in the optimized extraction solution of 100 mM sodium hydroxide and 1 mM tribasic sodium phosphate. All concentrations are in  $\mu\text{g/L}$ .

Initial Arsenic		Recovered Arsenic					
Nominal	Measured	Replicate	Replicate	Replicate	Replicate	Average	Std. Dev.
0	0.013	0.096	0.048	0.054	0.090	0.072	0.024
10	10.743	4.944	5.358	5.181	4.989	5.118	0.190
50	52.304	24.933	24.690	23.415	26.184	24.806	1.135
100	105.106	46.854	46.377	46.962	44.427	46.155	1.180
500	512.601	162.537	156.096	154.392	151.740	156.191	4.595
1000	1058.757	316.920	317.250	312.654	326.049	318.218	5.624

Table S-4: Initial and recovered arsenic concentrations for arsenic adsorbed from High Mix test solutions, as defined in the main article text, recovered from iron oxide xerogels after dry storage for 124 days and extraction in the optimized extraction solution of 100 mM sodium hydroxide and 1 mM tribasic sodium phosphate. All concentrations are in  $\mu\text{g/L}$ .

Initial Arsenic		Recovered Arsenic					
Nominal	Measured	Replicate	Replicate	Replicate	Replicate	Average	Std. Dev.
0	0.026	0.051	0.009	0.051	0.054	0.041	0.022
10	11.254	4.467	5.259	5.082	5.217	5.006	0.367
50	52.533	21.987	23.052	22.644	22.311	22.499	0.456
100	107.471	39.285	41.286	40.881	41.706	40.790	1.058
500	508.955	136.077	136.047	139.860	135.495	136.870	2.011
1000	1037.315	260.199	265.521	263.616	269.970	264.827	4.075

## S8 Xerogel bill of materials and cost calculation

Table S-5: Bill of materials for iron oxide xerogel fabrication reagents and estimated reagent cost for large-scale xerogel production. Xerogel recipe is adapted from Gash *et al.*<sup>2</sup> and Juhl *et al.*<sup>3</sup> as described in the main article text. Xerogel yield is the average of three syntheses after drying at room temperature. Bulk reagent suppliers and catalog numbers were selected for the lowest unit cost while maintaining desired reagent quality, with iron chloride hexahydrate quality maintained by using the largest available volume of the reagent which was used for the synthesis in this work. Listed prices are accurate as of June 2019, do not include an academic discount, and assume an Industrial Alcohol User Permit to avoid the cost of US alcohol excise tax on the ethanol used in the synthesis.

Component	Quantity				Bulk Reagents					Cost per g xerogel (USD/g)
	Fabrication	Solvent Exchange	Total	Total per g xerogel	Supplier	Catalog Number	Quantity	Cost (USD)	Unit Cost (per g or mL)	
FeCl <sub>3</sub> · 6 H <sub>2</sub> O (g)	6.487		6.487	2.416	Sigma-Aldrich	31232-6X1KG	6 kg	1100	0.183	0.44
Ethanol (mL)	52.5	250	302.5	112.6	Fisher Scientific	04-355-600	208 L	1331	0.006	0.72
Propylene oxide (mL)	18.06		18.06	6.725	Sigma-Aldrich	110205-18L-KL	18 L	415	0.023	0.16
Xerogel yield (g)	2.685									<b>1.32</b>



## References

- [1] S. Dixit and J. G. Hering, *Environmental Science & Technology*, 2003, **37**, 4182–4189.
- [2] A. E. Gash, T. M. Tillotson, J. H. Satcher Jr., J. F. Poco, L. W. Hrubesh and R. L. Simpson, *Chemistry of Materials*, 2001, **13**, 999–1007.
- [3] S. J. Juhl, N. J. Dunn, M. K. Carroll, A. M. Anderson, B. A. Bruno, J. E. Madero and M. S. Bono Jr., *Journal of Non-Crystalline Solids*, 2015, **426**, 141–149.
- [4] E. Arifin, J. Cha and J.-K. Lee, *Bulletin of the Korean Chemical Society*, 2013, **34**, 2358–2366.
- [5] S. Kong, Y. Wang, H. Zhan, S. Yuan, M. Yu and M. Liu, *Water Environment Research*, 2014, **86**, 147–155.
- [6] G. Limousin, J.-P. Gaudet, L. Charlet, S. Szenknect, V. Barthes and M. Krimissa, *Applied Geochemistry*, 2007, **22**, 249–275.
- [7] G. P. Jeppu and T. P. Clement, *Journal of Contaminant Hydrology*, 2012, **129**, 46–53.
- [8] D. C. Montgomery, G. C. Runger and N. F. Hubele, *Engineering Statistics*, John Wiley & Sons, Hoboken, New Jersey, USA, 3rd edn., 2004.
- [9] A. N. Kolmogorov, *Doklady Akademii Nauk USSR*, 1941, **31**, 99–101.
- [10] M. A. Gorokhovski and V. L. Saveliev, *Physics of Fluids*, 2003, **15**, 184–192.
- [11] T. Martin, C. Brockhoff and J. Creed, *Method 200.7, Revision 4.4: Determination of Metals and Trace Elements in Water and Wastes by Inductively Coupled Plasma-Atomic Emission Spectrometry*, U.S. Environmental Protection Agency, 1994.